International Journal of Circuit Theory and Applications

Design of Robust Digitally Controlled DC-DC Converters in the Presence of Strong Interference

Journal:	*International Journal of Circuit Theory and Applications*
Manuscript ID	CTA-16-0176.R1
Wiley - Manuscript type:	Research Article
Date Submitted by the Author:	26-Sep-2016
Complete List of Authors:	Hayes, Brendan; Dublin City University, Electronic Engineering Condon, Marissa; dublin city university, Giaouris, Damian; Newcastle University
Keyword:	bifurcation, chaos, intermittent operation, dc-dc converters, controller design, noise, intermittency

Design of Robust Digitally Controlled DC-DC Converters in the Presence of Strong Interference

Brendan Hayes*, Marissa Condon* and Damian Giaouris**

* School of Electronic Engineering, Dublin City University, Ireland.
The Rince Institute, Researching Innovative Engineering Technologies.

** School of Electrical and Electronic Engineering, Newcastle University, UK.

Abstract

One of the main advantages of digital control is the ability to design more sophisticated control strategies to enable high performance dc-dc converters. One such example is a buck converter operating with a digital state-feedback controller. Previous works characterise the nonlinear dynamics of such systems under ideal operating conditions. However, in practical applications, these conditions cannot be guaranteed. The focus of this work is on the behaviour of such systems when they operate in the presence of strong interference signals. Previous works on the effect of noise have shown that intermittent operation is possible when the frequency of the noise signal is close to the switching frequency. Intermittent operation can be characterised by long periods of stable operation interspersed with periods of unstable or chaotic operation which greatly downgrade the efficiency and performance of the converter and reduce its lifetime as for example increase the current ripple or add extra AC components at its output. Typically, such behaviour is avoided by modifying the circuit parameters. However, little or no work exists on developing design guidelines in order to effect its elimination. This is the focus of this research, that is, by utilising Filippov's theory on discontinuous differential equations, to set out a design procedure that can be applied to any dc-dc converter, to tune its controller in order to eliminate intermittent operation. As a case study, the digitally controlled buck converter with a state-feedback control law is selected.

Keywords: bifurcation; chaos; intermittent operation; dc-dc converters; controller design; noise.

1 Introduction

State of the art circuits for regulation employ digital control schemes owing to their advantages such as low power, immunity to analog component variations and the possibility for more advanced control schemes [1]. Digital state-feedback control is employed when high/optimal performance is required [2]. While several recent papers [2]–[4] have addressed the nonlinear dynamics of these circuits under ideal operating conditions, the focus of the current work is on their behaviour when they are perturbed by noise signals. The effect of the noise signals can be catastrophic as it may lead to permanent or intermittent unstable operation of the converter that will result in high current ripple or operation at unwanted voltage/current levels. Obviously, when a state feedback controller is used in state of the art applications that require fast and efficient performance, these phenomena are even more critical. The analysis of intermit operation is a much more complicated problem (as there is no steady-state fixed point in the system which can be used to perform standard bifurcation analysis) and this will be the focus of this work. In particular, our goal is to set out a design procedure in order to ensure stable operation.

Intermittent operation can be qualitatively described as distributed periods of irregular motion such as bursts of unstable or chaotic operation separated by long periods of stable operation [5]. It is a phenomenon that is frequently observed in periodically driven nonlinear systems, like the buck converter, where the frequency of a coupled signal is not consistent with the driving frequency of the system. It occurs when a crucial parameter is being modulated by the coupling signal. Such intermit operation has been observed in switch-mode power supplies which are not protected against spurious signals or where parasitic inductances or capacitances are present causing unwanted oscillations of a control signal [5]. These unwanted oscillations affect the efficiency of the system [6]–[8] and thus, a better analysis of their nonlinear dynamics is required to provide design guidelines in order to eliminate this type of operation.

Intermittent operation was first observed in dc-dc converters in [7]. By considering a Voltage-Mode Control (VMC) buck converter with the ramp signal being perturbed by a disturbance signal, the output voltage is seen to go through distributed periods of irregular motion. As the strength of the

interference signal increases, the duration of the unstable operation increases until the output is chaotic. While no quantitative analysis is performed, the author concludes that systems with high feedback gains are more likely to exhibit intermittent operation. In [8], the author considers perturbing the control signal of a VMC buck converter. Intermittent operation is observed when the frequency of the interference signal is close to the clock frequency or its rational multiples. In order to perform bifurcation analysis, a transformation that relates changes in time to changes in another variable is performed. This enables the derivation of an iterative discrete-time map and allows the examination of the eigenvalues of the system as a parameter varies. Similar work is carried out in [6] where sinusoidal, triangular and saw-tooth disturbance signals perturbing the input voltage, control voltage and reference voltage are considered. Other works qualitatively assessing the effect of spurious signals on dc-dc converters are in [9]–[14] and references therein.

Some of these previous works utilise iterative discrete-time maps to derive the Jacobian matrix. This method is algebraically complex and not suited to deriving conditions to tune a controller in order to avoid intermittent operation. The Filippov method is a technique that achieves the same objective as the work in [6] and [8] but in a more straightforward way, that is, to derive the Jacobian of the Poincaré map in order to assess the eigenvalues of the system. This technique has been used to assess the eigenvalues of the buck converter [15], predict the onset of period-doubling bifurcations in a PI controlled buck converter [16] and to develop stability criteria in order to tune a PID controlled buck converter [17]. Furthermore, little work has been carried out in the way of control of intermittent operation. [13] applies resonant parametric perturbation, where a control parameter is perturbed in order to ensure stability, to a parallel-buck converter. However, little or no work exists on design procedures for controllers in order to eliminate intermittent operation.

The aim of this research is to study the effect of noise perturbing the input voltage of a buck converter operating with a digital state-feedback controller and to develop a design procedure in order to ensure stable operation. This design procedure can be applied to any controller by modifying the relevant steps.

2 System Description

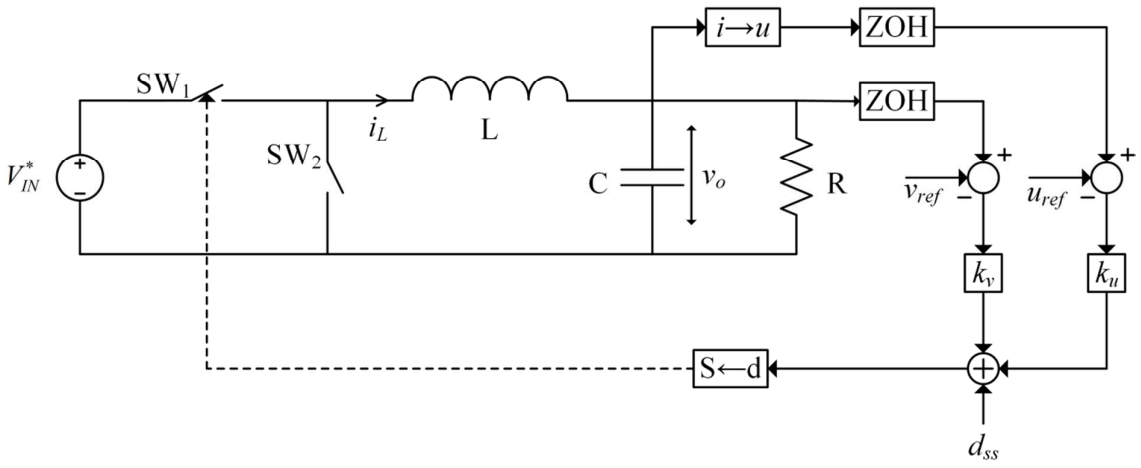

Fig. 1: Digital state-feedback buck converter with parameters L = 20 mH, C = 47 µF, R = 22 Ω, T = 400 µs, v_{ref} = 12.4381 V, u_{ref} = 11.677 V, k_v = -0.1334, k_u = 0.0092.

Figure 1 shows a buck converter controlled by an affine static digital state-feedback control law. The purpose of the buck converter is to step an input voltage, V_{IN}^*, to a lower output voltage, v_o, where $v_o = dV_{IN}^*$ and d is the duty cycle of switch SW_1. SW_1 is closed at the start of the switching period for a time dT and is open for the remainder of the switching period, $(1\text{-}d)T$, where T is the switching period of the buck converter and SW_1 and SW_2 open and close with a frequency of $f = 1/T$. SW_2 operates complimentary to SW_1. Hence, the open loop buck converter model is written as:

$$\frac{d}{dt}\begin{bmatrix} v_o \\ i_L \end{bmatrix} = \begin{bmatrix} -\frac{1}{RC} & \frac{1}{C} \\ -\frac{1}{L} & 0 \end{bmatrix}\begin{bmatrix} v_o \\ i_L \end{bmatrix} + \delta\begin{bmatrix} 0 \\ \frac{1}{L} \end{bmatrix} V_{IN}^* \tag{1}$$

where δ = 1 when SW_1 is closed and 0 when open. Instead of the inductor current, i_L, it is easier to consider a new variable u, where u is a linear combination of the two state variables, $u = \frac{1}{\omega C} i_L - \frac{\sigma}{\omega} v_o$, in order to simplify the equations [18]. Letting $x = [v_o \;\; u]^T$, (1) becomes:

$$\frac{dx}{dt} = \begin{bmatrix} -\sigma & \omega \\ -\omega & -\sigma \end{bmatrix} x + \delta\begin{bmatrix} 0 \\ \delta_U \end{bmatrix} V_{IN}^* \tag{2}$$

where $\sigma = 1/2RC$, $\omega = \sqrt{1/LC - \sigma^2}$ and $\delta_U = \left(\omega^2 + \sigma^2\right)/\omega$. As a digital state-feedback controller is used, the state vector is sampled at the switching frequency, using a Zero-Order Hold (ZOH), and compared to the demanded value:

$$x_{ref} = [v_{ref} \;\; u_{ref}]^T + [\Delta v_o \;\; \Delta u \;\;]^T$$

where Δv_o and Δu are the estimated ripple of the state variables given by [19]:

$$\Delta v_o = \frac{\Delta i_L T}{8C}$$

$$\Delta u = \frac{V_{IN}^* - v_{ref}}{\omega LC}\left(1 - \frac{\sigma T}{8}\right)dT$$

By knowing the circuit parameters and estimating the ripple of the state variables, this allows for the proper selection of the x_{ref} terms meaning the control scheme has an indirect integral action. The state-feedback control law is formed by adding the two state error terms together, comparing them to the demanded values and multiplying by the gain $\left[k_v \;\; k_u\right]$, as well as adding a constant affine term equal to the desired steady-state value of the system $d_{ss} = v_{ref}/V_{IN}^*$. The control signal is given by:

$$d(kT) = \left[k_v \;\; k_u\right]\left(x(kT) - x_{ref}\right) + d_{ss} \tag{3}$$

Figure 2 shows (a) the steady state output voltage and (b) the Poincaré section of the buck converter operating under ideal conditions. The Poincaré section samples the state variables at the switching frequency and plots one state variable against another. If the system is operating with a period-1 orbit, only one point will be seen which is the fixed point of the Poincaré map. If the system is operating with a period-*n* orbit then the trajectory intersects the Poincaré section *n* times. The effect of perturbing the input voltage with an undesirable noise signal is now considered.

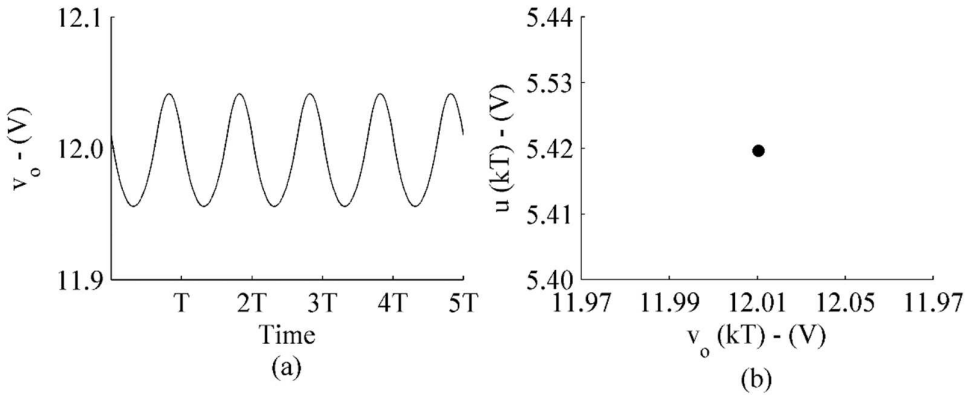

Fig. 2: (a) Steady-state output voltage of buck converter (b) Poincaré section.

3 Perturbation of Input Voltage

The system described in (2) and (3) has been modelled and shown to be stable for the circuit parameters in Fig. 1. These simulations assume ideal operating conditions and ideal sources. However, noise sources can affect the input voltage of the buck converter. Typically, these are caused by finite input capacitances, the ESR of the input capacitor or stray inductance and stray capacitance in the circuit [20]. Consider an interference signal, v_s, which is injected directly into the input voltage of the converter. This coupling can be modelled as an additive process which superposes the disturbance directly on the input voltage. The perturbed input voltage V_{IN} is now given by:

$$V_{IN} = V_{IN}^* + v_s \tag{4}$$

If the interference signal is periodic, the simplest case to consider is a sinusoidal disturbance with an amplitude $\hat{v}_s$ and frequency f_n. Then the perturbed signal is:

$$V_{IN} = V_{IN}^* + \hat{v}_s \sin\left(2\pi f_n t\right) = V_{IN}^* \left(1 + \alpha_v \sin\left(2\pi f_n t\right)\right) \tag{5}$$

where α_v is the strength of the interference signal which is defined as the ratio of $\hat{v}_s$ to V_{IN}^* i.e. $\alpha_v = \hat{v}_s / V_{IN}^*$ and $f_n = \alpha_f f$ where α_f is the ratio of the noise frequency to the switching frequency. Since the noise signal is coupled unintentionally, it is possible that the frequency of the noise will be close to the switching frequency. In order to determine what period the output is and the intermittent

behaviour, the output voltage is sampled once per switching cycle and plotted against the time instant. This type of diagram is known as a time-bifurcation diagram and illustrates the change in behaviour of the system as time varies as opposed to the conventional parameter-bifurcation diagram. Figures 3-5 show the resulting time-bifurcation diagrams for $f_n = 2501$ (Hz), 2499 (Hz) and 5001 (Hz) for varying signal strengths. From these plots, the following observations can be made:

- For low signal strengths, $\alpha_v = 0.16$, the converter maintains the expected period-1 orbit, though the operating point fluctuates due to the oscillating input voltage. The effect of the disturbance signal is not significant and no intermittent operation is present. Figures 3-5 (a) shows the corresponding time-bifurcation plots.
- As the strength of the interference signal increases, the system cannot maintain the expected period-1 orbit. Instead, the system operates with a period-1 orbit for the majority of the time with bursts of unstable operation. The system loses stability through a Hopf bifurcation and a limit cycle is present on the output. However, the system does regain stability after a short period of time. This type of behaviour is known as intermittent operation. Figures 3-5 (b) shows the corresponding time-bifurcation diagrams.
- Further increases to the strength of the disturbance signal leads to an increase in the proportion of time over which the limit cycle is present as well as an increase in its amplitude. The corresponding time-bifurcation diagrams are plotted in Figs. 3-5 (c) and (d).

While any noise frequency can lead to intermittent operation, noise frequencies close to the switching frequency are more likely to cause intermittent operation. This is due to the length of time spent in the unstable region for differing noise frequencies.

Consider the case where the input to the system is not being perturbed. Figure 6 shows the bifurcation diagram with V_{IN}^* as the bifurcation parameter. The system is seen to undergo a bifurcation at $V_{IN}^* = 29$ (V), term this value $V_{IN\_crit}^*$. If a stable V_{IN}^* value is selected and the system is perturbed by some sinusoidal disturbance signal, the following sequence of events occurs for sufficiently large interference signals:

- At $t = 0$, the system is stable.
- V_{IN} increases and reaches the point where $V_{IN} = V^*_{IN\_crit}$ at $t = t_{crit}$. The system is operating in the unstable region.
- The system remains unstable until $V_{IN} = V^*_{IN\_crit}$ is reached again at $t = t_{stab}$.
- The system will repeat with a period of $T_{\text{int}} = 1/|f_n - f|$.

It is important to note that in a time-bifurcation plot, there is only one switching period between each sampling point. Thus, the system may appear to be stable for several iterations past t_{crit}. However, closer inspection of the eigenvalues may reveal that the system is unstable.

For values of f_n close to the switching frequency, the intermittent period is large e.g. for $f_n = 2501$ (Hz), $T_{\text{int}} = 1$ (s). The length of time the system spends in the unstable region is quite long i.e. $t_{stab} - t_{crit}$. The system spends enough time in the unstable region for intermittent operation to be observed on a time-bifurcation diagram, as in Figs. 3-5 (b)-(d).

For values of f_n further away from the switching frequency, the intermittent period is much shorter e.g. for $f_n = 2600$ (Hz), $T_{\text{int}} = 0.01$ (s). The time spent in the unstable region is 100$^{\text{th}}$ of that when $f_n = 2501$ (Hz). While the system is unstable every 0.01 (s), this is not captured by a time-bifurcation diagram. The system is intermittently unstable but does not exhibit intermittent operation as the system does not spend a sufficiently long enough period of time in the unstable region for the systems trajectory to noticeably diverge from the fixed point. Hence, frequencies close to the switching frequency are studied in this work as they are more likely to exhibit intermittent operation.

We will now consider using the Filippov method as a tool to assess the stability of the described operation and track the eigenvalues of the system as its trajectory evolves.

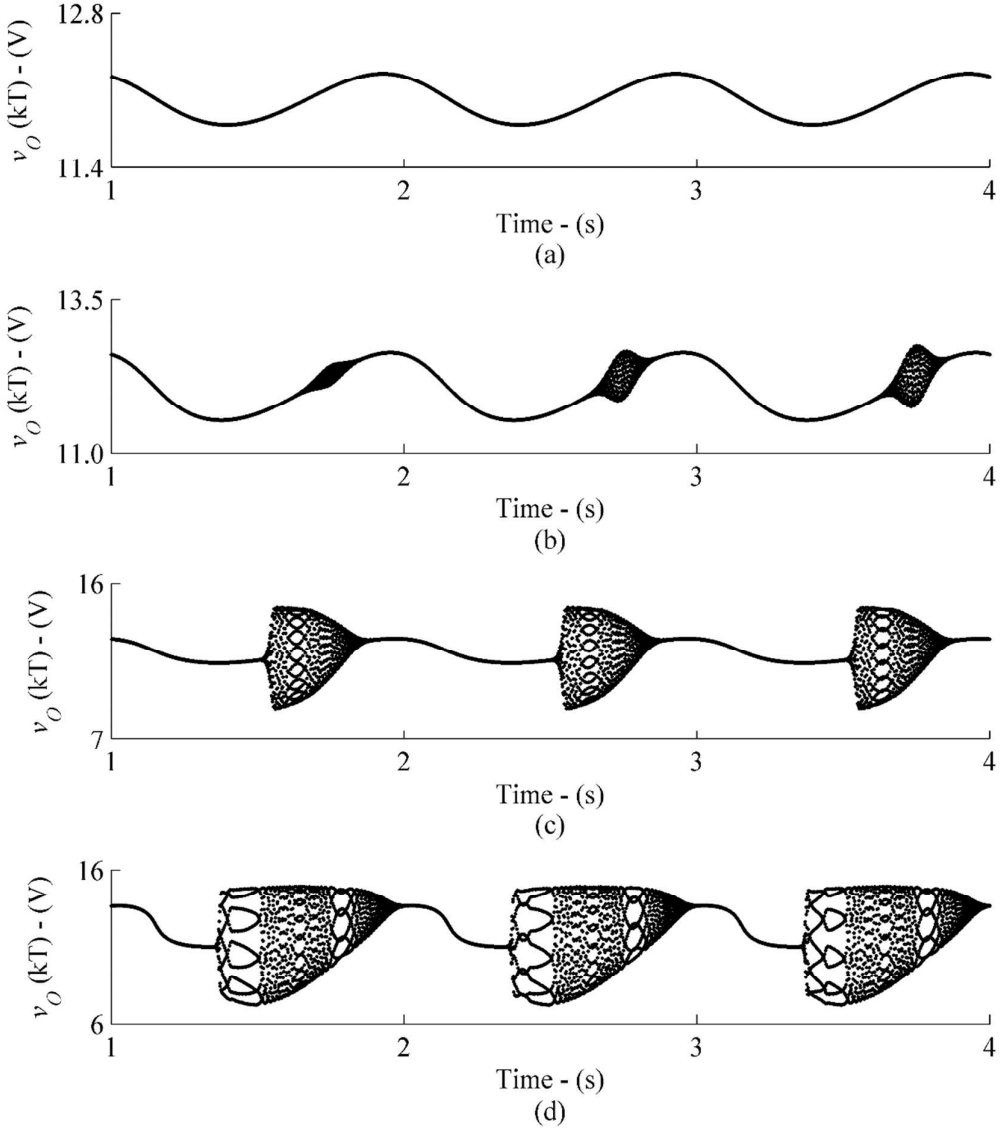

Fig. 3: Time-bifurcation diagrams with a sinusoidal interference signal with a frequency of $f_n = 2501$ (Hz) for (a) $\alpha_v = 0.16$ (b) $\alpha_v = 0.38$ (c) $\alpha_v = 0.5$ and (d) $\alpha_v = 1$.

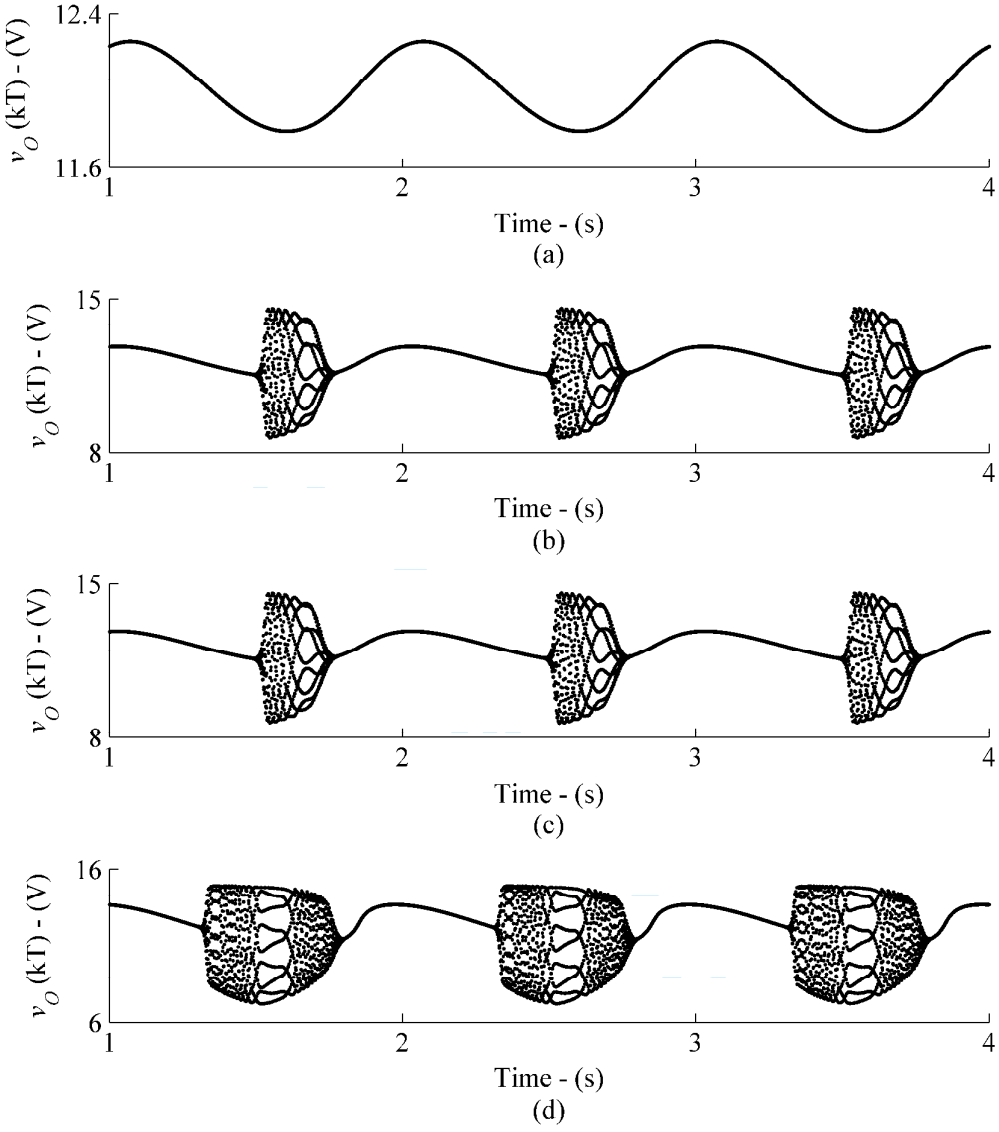

Fig. 4: Time-bifurcation diagrams with a sinusoidal interference signal with a frequency of $f_n = 2499$ (Hz) for (a) $\alpha_v = 0.16$ (b) $\alpha_v = 0.38$ (c) $\alpha_v = 0.5$ and (d) $\alpha_v = 1$.

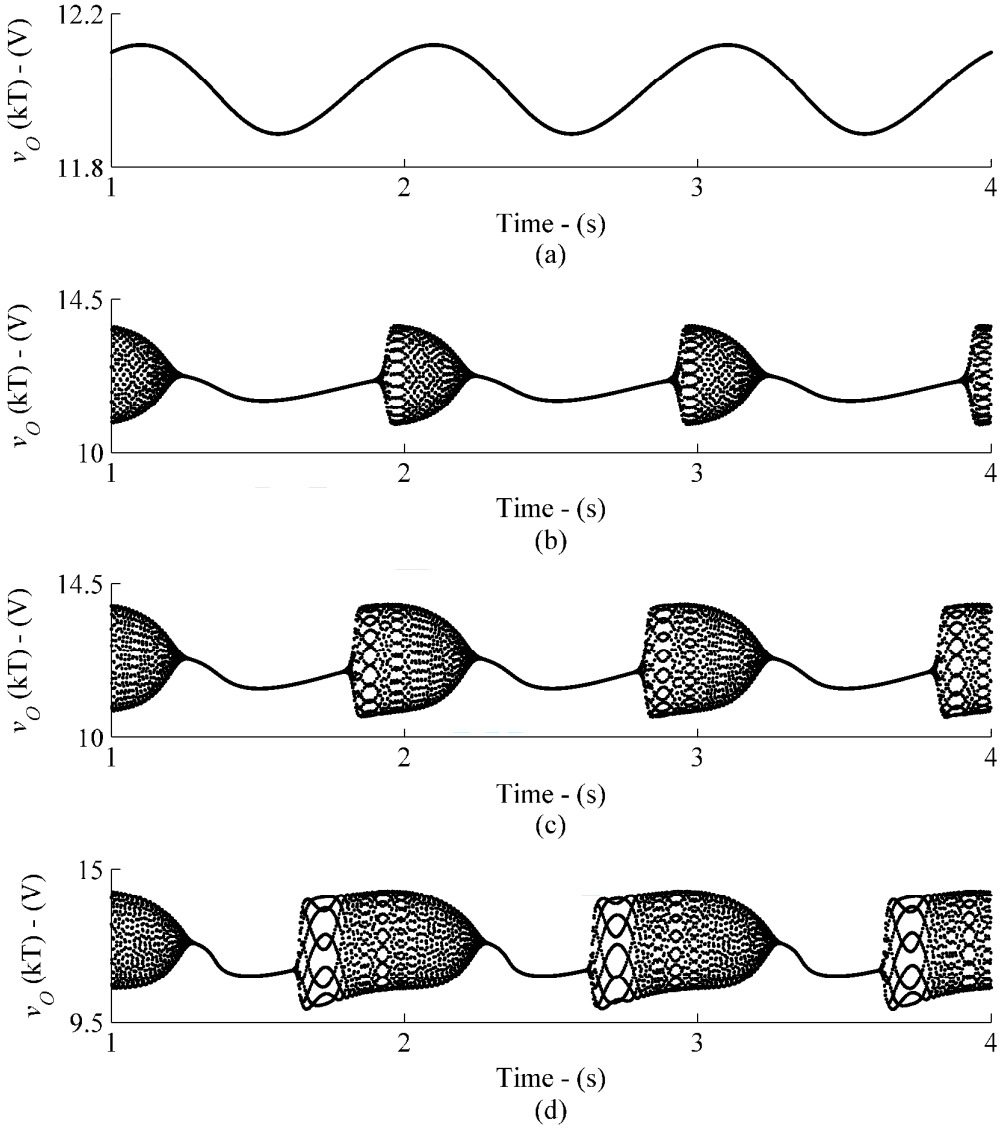

Fig. 5: Time-bifurcation diagrams with a sinusoidal interference signal with a frequency of $f_n = 5001$ (Hz) for (a) $\alpha_v = 0.16$ (b) $\alpha_v = 0.50$ (c) $\alpha_v = 0.57$ and (d) $\alpha_v = 1$.

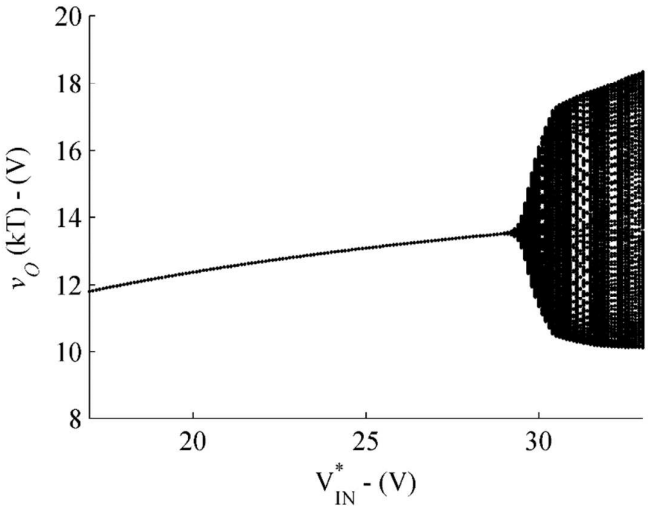

Fig. 6: Bifurcation diagram of digital state-feedback buck converter with V^*_{IN} as the bifurcation parameter.

4 Stability Analysis

As there is no steady-state fixed point in the system which can be used to perform bifurcation analysis of the time-bifurcation plots above, a transformation must take place. The transformation must convert changes in time to changes in another variable. This enables stability analysis to be performed on a parameter-bifurcation plot. The new parameter, ϕ, is considered as a conceptual phase shift to model the equivalent drift of the system from the switching frequency and the perturbed input voltage can now rewritten as:

$$V_{IN} = V^*_{IN}\left[1+\alpha_v \sin\left(2\pi ft+\phi\right)\right] \tag{6}$$

where $\phi = 2\pi\left|f - f_n\right|t$. Using (6), the time-bifurcation plots presented in Figs. 3-5 can be reconstructed as parameter-bifurcation plots with ϕ as the bifurcation parameter. Figure 7 shows the reconstructed parameter-bifurcation plots for $f_n = 2501$ (Hz). When the time-bifurcation plots and the parameter-bifurcation plots are compared, the results are in very close agreement. This transformation enables standard-bifurcation techniques to be used to analyse the stability of the system. Essentially, the parameter-bifurcation diagram over the range $0 \le \phi \le 2\pi$ is the same as the time-bifurcation diagram over the intermittent period, T_{int}, shown in Figs. 3-5. The Filippov method is

now used to derive the Monodromy matrix which enables the stability of the system to be assessed as ϕ varies. The results can then be converted from the parameter-domain to the time-domain. For brevity, the case for $f_n = 2501$ (Hz) will be presented in this section. However, the proposed method can be extended to any value of the noise frequency.

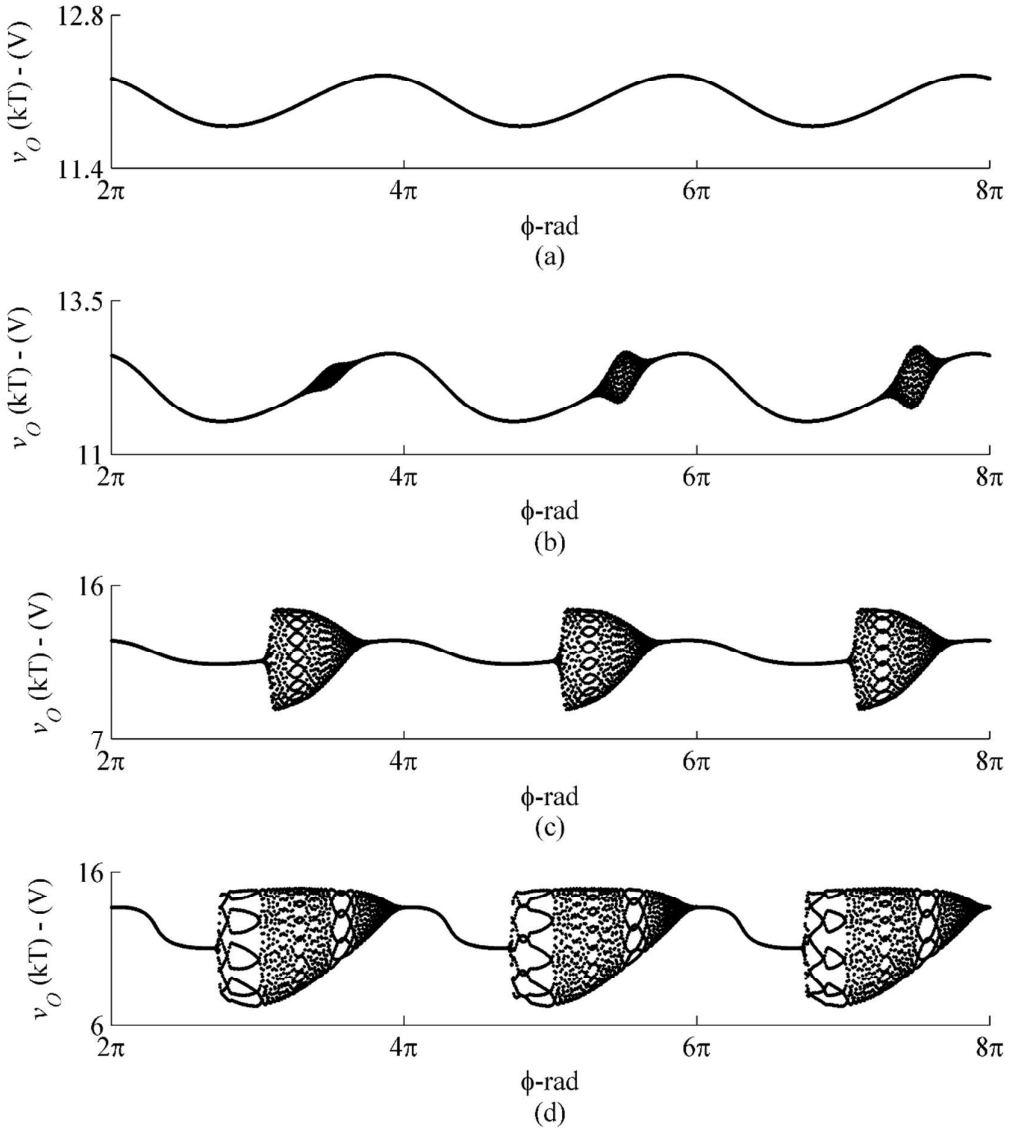

Fig. 7: Parameter bifurcation diagram with a sinusoidal interference signal with $f_n = 2501$ (Hz) for (a) α_v = 0.16 (b) α_v = 0.38 (c) α_v = 0.5 and (d) α_v = 1.

The stability of a general orbit, say $x(t)$, is assessed by placing a small perturbation at $t = t_0$ and monitoring the evolution of the perturbation $\Delta x(t)$. The evolution is related to the initial perturbation by the fundamental solution matrix $\Phi(t, t_0)$ and when the vector field governs the original orbit is linear time invariant, the fundamental solution matrix is given by the exponential matrix:

$$\Delta x(t) = \Phi(t, t_0)\Delta x(t_0) = e^{A(t-t_0)}\Delta x(t_0) \tag{7}$$

If the orbit is periodic, then the stability can be quantitatively determined by the eigenvalues of the fundamental solution matrix evaluated at $t = t_0 + T$, where T is the period of the orbit under study. The fundamental solution matrix obtained at $t = t_0 + T$ is termed the Monodromy matrix whose eigenvalues are called Floquet Multipliers. If the Floquet Multipliers lie inside the unit circle, the orbit is stable.

The buck converter switches between two topologies and each is described by a linear vector field:

$$\dot{x} = A_j x + B_j x_{in}, j \in \{1, 2\} \tag{8}$$

where j denotes the topology when SW_1 is closed and open. Due to the switching of topologies, (7) cannot be assessed directly. Instead, the method shown in [21] must be applied. The effect the switching has on the perturbation vector is given by:

$$\Delta x(t_+) = S\Delta x(t_-) \tag{9}$$

where t_- and t_+ denote the times just before and after switching between topologies. The Saltation matrix, S, is given by [15]:

$$S = I + \left.\frac{(f_+ - f_-)n^T}{n^T f_- + \frac{\partial h}{\partial t}}\right|_{\substack{t=(k+d)T \\ x(t)=x(t_\Sigma)}} \tag{10}$$

with f_- and f_+ being the right hand side of (2) before and after switching respectively, $h(x,t)$ is the switching surface and n is the normal vector to the switching surface. Thus, the perturbation at the end

of the switching period related to that at the beginning of the switching period is given by the Monodromy matrix:

$$\Phi_M(T,0) = S_2\Phi_{OFF}S_1\Phi_{ON} \tag{11}$$

S_1 relates to the first switching event at $t = dT$ and S_2 relates to the second switching event at $t = T$. The stability of the system is found by finding the eigenvalues of (11). If all of the eigenvalues lie inside the unit circle, the system is asymptotically stable. The elements of (10) for this work are:

$$f_- = \begin{bmatrix} -\sigma v_\Sigma + \omega u_\Sigma \\ -\omega v_\Sigma - \sigma u_\Sigma + \delta_U V_{IN} \end{bmatrix},\ f_+ = \begin{bmatrix} -\sigma v_\Sigma + \omega u_\Sigma \\ -\omega v_\Sigma - \sigma u_\Sigma \end{bmatrix} \tag{12}$$

$$h(x,t) = d_{ss} + \begin{bmatrix} k_v & k_u \end{bmatrix}\left(x(kT) - x_{ref}\right) - t \bmod T \tag{13}$$

(13) is dependent on the state variables at $t = kT$ but n and $\partial h/\partial t$ are both evaluated at the switching instant i.e. $t = (k+d)T$. As shown in Appendix A, the state vector at start of the switching period can be rewritten in terms of the state vector at the switching instant. Thus, $h(x,t)$ becomes:

$$\begin{aligned} h(x,t) = \ d_{ss} + \begin{bmatrix} k_v & k_u \end{bmatrix}\Big(e^{-AdT}x\big((k+d)T\big) + A^{-1}\left(e^{-AdT} - I\right)BV_{IN}^* \\ + \alpha_v N_{kT} BV_{IN}^* - x_{ref}\Big) - t \bmod T \end{aligned} \tag{14}$$

where:

$$\begin{aligned} N_{kT} = \left(A^2 + (2\pi f_n)^2\right)^{-1} \ \big(-AI\sin(2\pi f_n kT) - 2\pi f_n I\cos(2\pi f_n kT) \\ + Ae^{-AdT}\sin(2\pi f_n(k+d)T) + 2\pi f_n e^{-AdT}\cos(2\pi f_n(k+d)T)\big) \end{aligned}$$

n and $\partial h/\partial t$ are:

$$n = \left.\begin{bmatrix} \dfrac{\partial h}{\partial v_o} \\ \dfrac{\partial h}{\partial u} \end{bmatrix}\right|_{t=(k+d)T} = e^{\sigma dT}\begin{bmatrix} k_v\cos(\omega dT) + k_u\sin(\omega dT) \\ -k_v\sin(\omega dT) + k_u\cos(\omega dT) \end{bmatrix} \tag{15}$$

$$\left.\frac{\partial h}{\partial t}\right|_{t=(k+d)T} = e^{\sigma dT}\begin{pmatrix} \left((\sigma k_v + \omega k_u)\cos(\omega dT) + (\sigma k_u - \omega k_v)\sin(\omega dT)\right)v_\Sigma \\ \left((-\sigma k_v - \omega k_u)\sin(\omega dT) + (\sigma k_u - \omega k_v)\cos(\omega dT)\right)u_\Sigma \\ \left(k_v \sin(\omega dT) - k_u \cos(\omega dT)\right)\delta_U V_{IN} \end{pmatrix} - \frac{1}{T} \quad (16)$$

Evaluating (10) using (12), (15) and (16), S_1 is given as:

$$S_1 = \begin{bmatrix} 1 & 0 \\ S_{21} & 1+S_{22} \end{bmatrix} \quad (17)$$

where:

$$S_{21} = T\delta_U V_{IN} e^{\sigma dT}\left(k_v \cos(\omega dT) + k_u \sin(\omega dT)\right)$$
$$S_{22} = T\delta_U V_{IN} e^{\sigma dT}\left(-k_v \sin(\omega dT) + k_u \cos(\omega dT)\right)$$

The second switching point occurs at the falling edge of the ramp signal thus, S_2 is the identity matrix of the same dimension as S_1. The overall Monodromy is as follows:

$$\Phi_M = e^{A(1-d)T} S_1 e^{AdT} \quad (18)$$

where the exponential matrix is given by:

$$e^{At} = e^{-\sigma t}\begin{bmatrix} \cos(\omega t) & \sin(\omega t) \\ -\sin(\omega t) & \cos(\omega t) \end{bmatrix}$$

Figure 8 shows the parameter-bifurcation plots of the system with ϕ as the bifurcation parameter for varying signal strengths with $f_n = 2501$ (Hz). Consider the case when $\alpha_v = 0.5$. The corresponding parameter-bifurcation plot is shown in Fig. 8 (c). This can be broken into 3 regions:

1. $0 \leq \phi \leq 1.885$: In this region, the system is stable and operating with a period-1 orbit.
2. $1.885 \leq \phi \leq 4.964$: The system is unstable and undergoes a bifurcation at $\phi = 1.885$, this is confirmed by assessing the eigenvalues of (18) at the bifurcation point which are presented in Table 1. Since the $|\lambda| > 1$ and λ has a non-zero imaginary part, it is determined that a Hopf bifurcation takes place.
3. $4.964 \leq \phi \leq 6.28$: The system is stable and operating with a period-1 orbit.

Similar dynamics occur in Fig. 8 (b)-(d), where the system moves from a stable orbit to an unstable orbit through a Hopf bifurcation. In the next section, a design procedure to tune one of the feedback gains of the controller in order to avoid intermittent operation is presented.

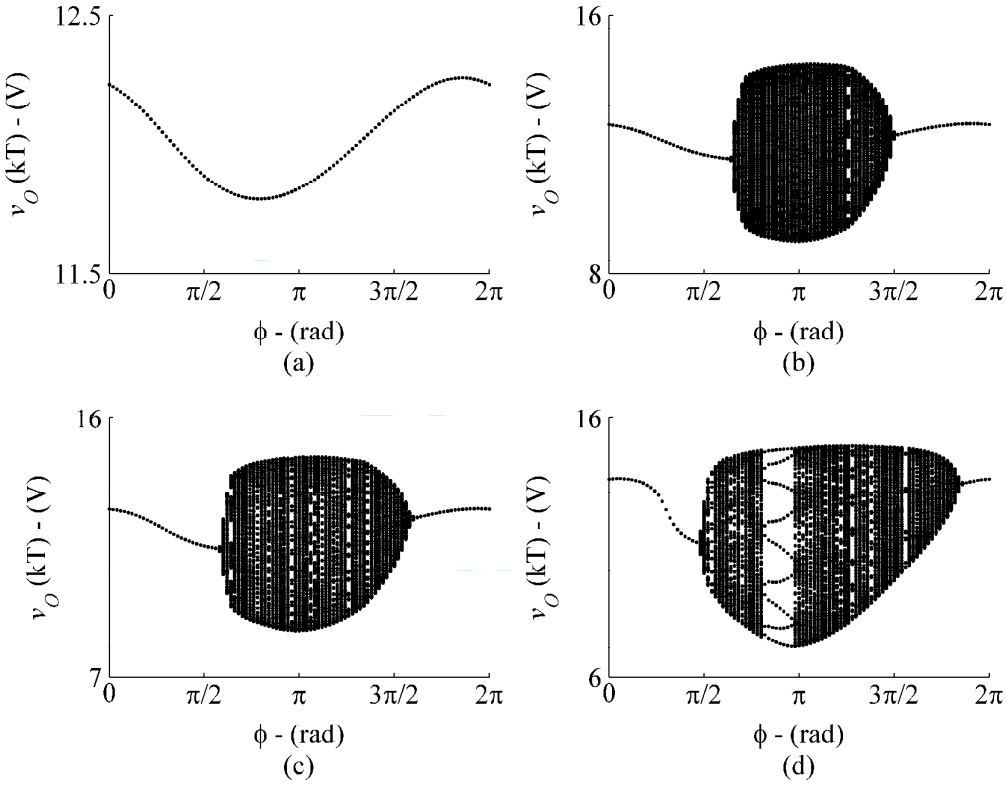

Fig. 8: Parameter-bifurcation diagram of ϕ with (a) $\alpha_v = 0.16$ (b) $\alpha_v = 0.38$ (c) $\alpha_v = 0.50$ and (d) $\alpha_v = 1.00$ for $f_n = 2501$ (Hz).

4.1 Design Procedure

In the previous section, by assessing the eigenvalues of the Monodromy matrix presented in (18), it was shown that the system undergoes a Hopf bifurcation as ϕ varies. This type of operation can be catastrophic in many applications and it must be avoided. In this section, we present a procedure that can be used to tune a control variable in any control scheme in order to avoid intermittent operation. As a case study, we will derive an expression to tune the k_u term of the digital state-feedback controller in order to eliminate intermittent operation.

Given a two-by-two matrix, the characteristic equation is given by [22]:

$$\lambda^2 - \mathrm{tr}\left(\Phi_M\right)\lambda + \det(\Phi_M) \tag{19}$$

The general solution to (19) is:

$$\lambda_{1,2} = \frac{tr\left(\Phi_M\right) \pm \sqrt{tr\left(\Phi_M\right)^2 - 4\det\left(\Phi_M\right)}}{2} \tag{20}$$

where tr and det are the trace and determinant of the Monodromy matrix given by:

$$tr(\Phi_M) = \underbrace{2e^{-\sigma T}\cos\left(\omega T\right)}_{M} + \underbrace{Te^{-\sigma(1-d)T}\delta_U\left(k_v\sin\left(\omega(1-d)T\right) + k_u\cos\left(\omega(1-d)T\right)\right)}_{P}V_{IN} \tag{21}$$

$$\det\left(\Phi_M\right) = e^{-2\sigma T} + Te^{-\sigma(2-d)T}\delta_U V_{IN}\left(-k_v\sin\left(\omega dT\right) + k_u\cos\left(\omega dT\right)\right) \tag{22}$$

Thus, the discriminant of (20) is given as:

$$tr\left(\Phi_M\right)^2 - 4\det\left(\Phi_M\right) = \left(\underbrace{4e^{-2\sigma T}\left(\cos^2\left(\omega T\right) - 1\right)}_{R} \underbrace{4e^{-\sigma(2-d)T}\delta_U T\left[k_v\sin\left(\omega T\right)\cos\left(\omega(1-d)T\right) - k_u\sin\left(\omega T\right)\sin\left(\omega(1-d)T\right)\right]}_{Q} V_{IN} \underbrace{\left[e^{-\sigma(1-d)T}\delta_U T\left(k_v\sin\left(\omega(1-d)T\right) + k_u\cos\left(\omega(1-d)T\right)\right)\right]^2}_{P^2} {V_{IN}}^2 \right)$$

The magnitude of (20) is given by:

$$|\lambda_{1,2}| = \sqrt{\left(\frac{M + PV_{IN}}{2}\right)^2 + \frac{-\left(P^2 V_{IN}{}^2 + QV_{IN} + R\right)}{4}} \tag{23}$$

Setting $|\lambda_{1,2}| = 1$ which is the condition for having a bifurcation, yields:

$$(2MP - Q)V_{IN} + \left(M^2 - R - 4\right) = 0$$

$$4e^{-\sigma(2-d)T}\delta_U T\left(-k_v \sin(\omega dT) + k_u \cos(\omega dT)\right)V_{IN} + 4e^{-2\sigma T} - 4 = 0 \tag{24}$$

Rearranging (24), the value of k_u at which a Hopf bifurcation takes place can be determined. This is termed k_{u_crit} or the critical k_u value and is given by:

$$k_{u\_crit} = \frac{1 - e^{-2\sigma T}}{e^{-\sigma(2-d)T}\delta_U T V_{IN} \cos(\omega dT)} + k_v \tan(\omega dT) \tag{25}$$

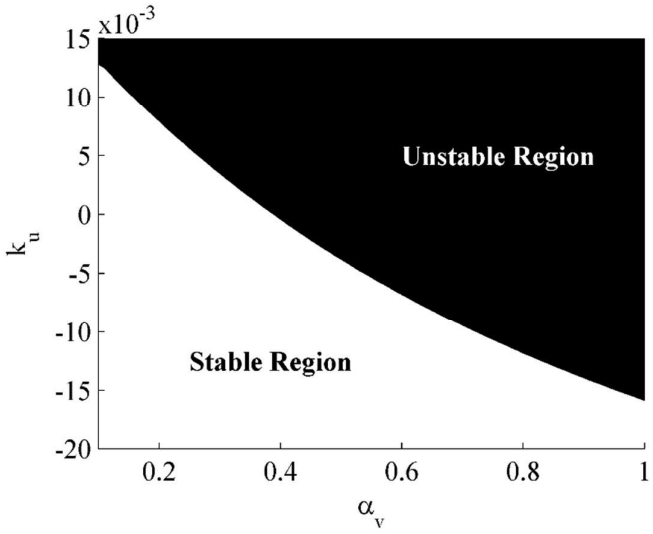

Fig. 9: Values of k_u at which intermittent operation occurs as α_v varies for $f_n = 2501$ (Hz).

Figure 9 shows the critical k_u value, calculated using (25), as the strength of the interference signal increases. When k_u is in the shaded region, the system is unstable. This can be used by designers in order to tune a digital state-feedback converter in order to avoid intermittent operation. Systems with high feedback gains are more likely to exhibit intermittent operation [7]. Thus, lower feedback gains are desirable. However, high feedback gains may be required in order to meet some desired response

characteristic. Since noise signals are unpredictable, ideally, a method of changing the gain term as the input voltage varies in such a way as to minimise the effect on the response characteristics while avoiding intermittent operation is required. In the next section a controller is proposed where the input voltage is monitored and the k_u term is updated appropriately using (25).

5 Controller Design

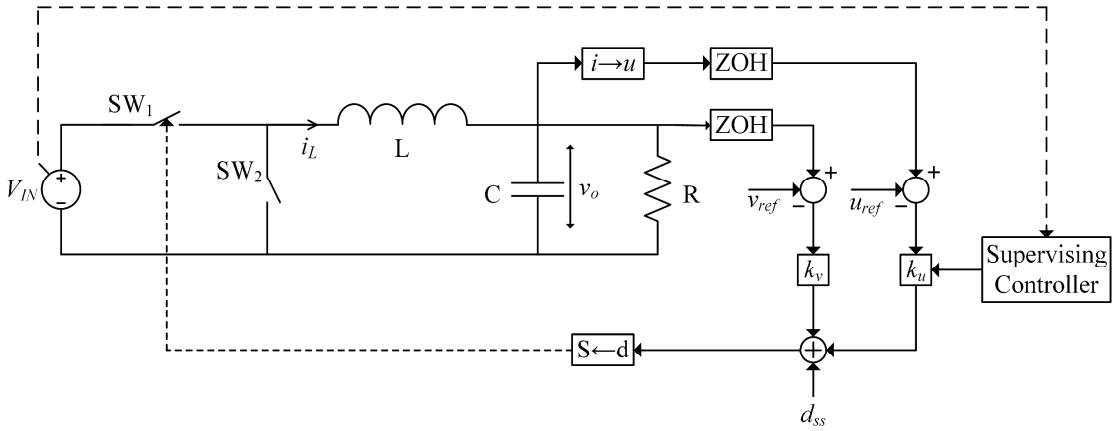

Fig. 10: Buck converter with an input voltage supervisory controller.

In the previous section, the Monodromy matrix was calculated and the Floquet multipliers were derived as a function of the controller parameters (25). A formula for calculating the value of k_u which leads to a Hopf bifurcation was developed (25). This enables the development of an adaptive state-feedback controller. By modifying (3) and using (25), an adaptive control scheme is proposed and illustrated in Fig. 10. In the suggested scheme, estimators are used to monitor the input voltage [23]–[25] and determine the amplitude and frequency of any noise source present at the input. The function of the supervising controller is to update the k_u term in order to avoid intermittent operation. This can ensure stable period-1 orbits. The controller operates as follows:

1. The supervising controller monitors the input voltage for disturbances. If no disturbances are present, the controller does not modify the control law.
2. When a disturbance is present, the controller identifies the amplitude and frequency of the interference signal.
3. The supervising controller checks if the system is stable. This is done by evaluating the eigenvalues of the Monodromy matrix presented in (18).
    a. If all of the eigenvalues over the range $0 \leq \phi \leq 2\pi$ lie inside the unit circle, the system is stable and k_u remains the same.

b. Otherwise, the system is unstable and the k_u term must be updated using (25) (or a figure similar to Fig. 9) to make the system stable again. Sample values of k_u are given in Table 2 which ensure stability for different noise frequencies.

Using this method the resulting time-bifurcation plots are illustrated in Figs. 11-13 with $f_n = 2501$ (Hz), 2499 (Hz) and 5001 (Hz), respectively. By determining the critical k_u value, the system can avoid intermittent operation and instead, operate with a stable period-1 orbit. While the fixed point of the system oscillates due to the periodic nature of the perturbed input voltage, the intermittent operation seen in Figs. 3-5, when the standard control law is used, is eliminated.

Load changes are frequent and important in power electronic systems as they can lead to unstable operation. The proposed method can take any parameter change into account through the Monodromy matrix which enables the derivation of the critical gain terms to ensure stable operation. In this work, fluctuations in the input voltage are considered while the load resistance is assumed to be fixed. Thus, it is important to demonstrate that the controller is robust to load variations. Figures 14-16 show the effect of a step increase in the load resistance. The system starts with $R = 22\Omega$ at $t = 0$ and a step increase occurs at $t = 2$ for four different increments of (a) 10% (b) 20% (c) 30% and (d) 40%. Since there is a step change in R at $t = 2$, a small disturbance is present as the system reacts to this change. The following observations can be made:

- For small changes in the load resistance, a 10% increase, the controller maintains the desired period-1 orbit. The system does not exhibit intermittent operation.
- When the load is increased by 20%, intermittent operation is observed for the first time. The amplitude of the unstable operation is quite small.
- For larger increases to the load resistance, the amplitude and period of the intermittent operation increases.

The tuning method presented in this paper can ensure stable period-1 orbits as the load varies up to a 20% increase to its nominal value. This method can be adapted for any controller type in order to avoid intermittent operation.

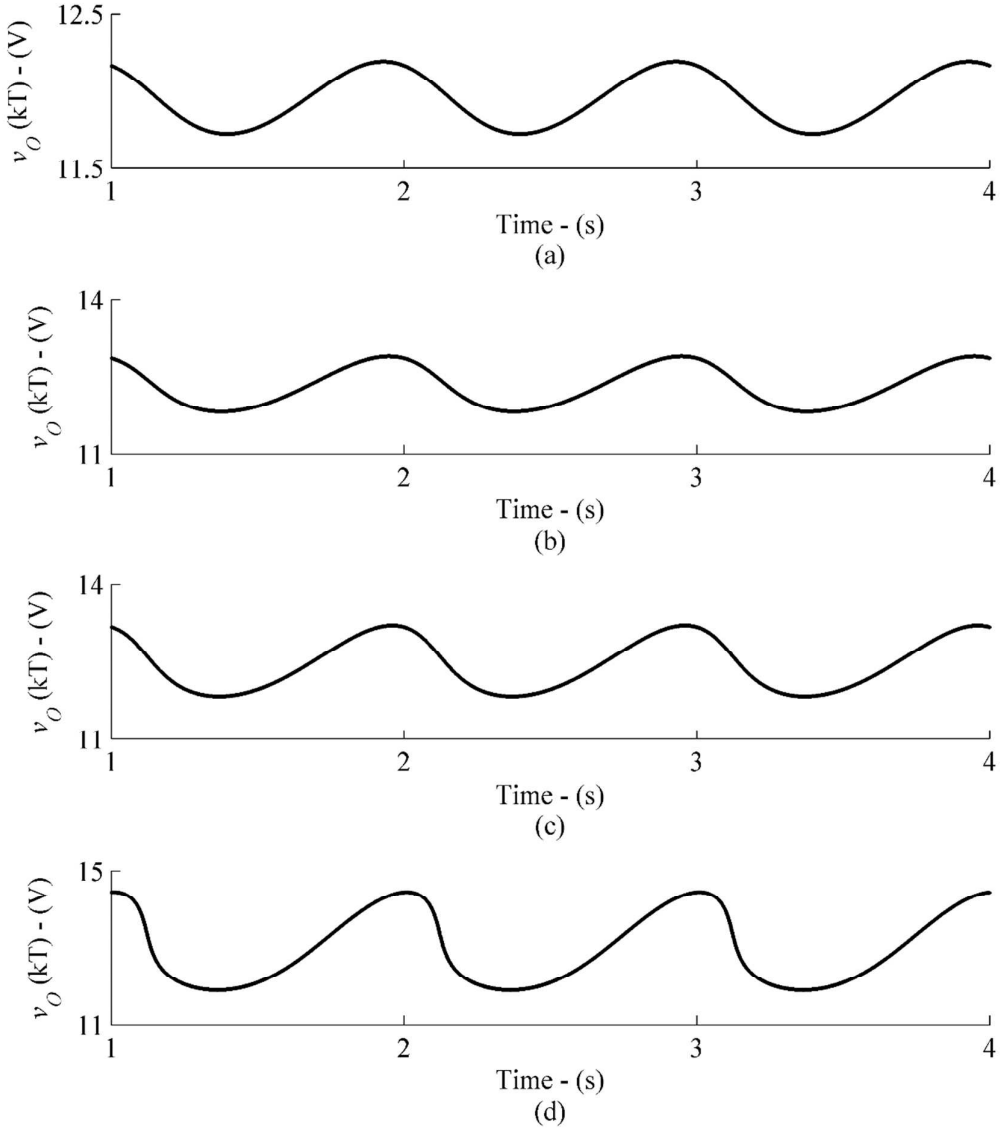

Fig. 11: Time-bifurcation plots of the output voltage for $f_n = 2501$ (Hz) using the k_u values presented in Table 2 (a) for (a) $\alpha_v = 0.16$ (b) $\alpha_v = 0.38$ (c) $\alpha_v = 0.5$ and (d) $\alpha_v = 1$.

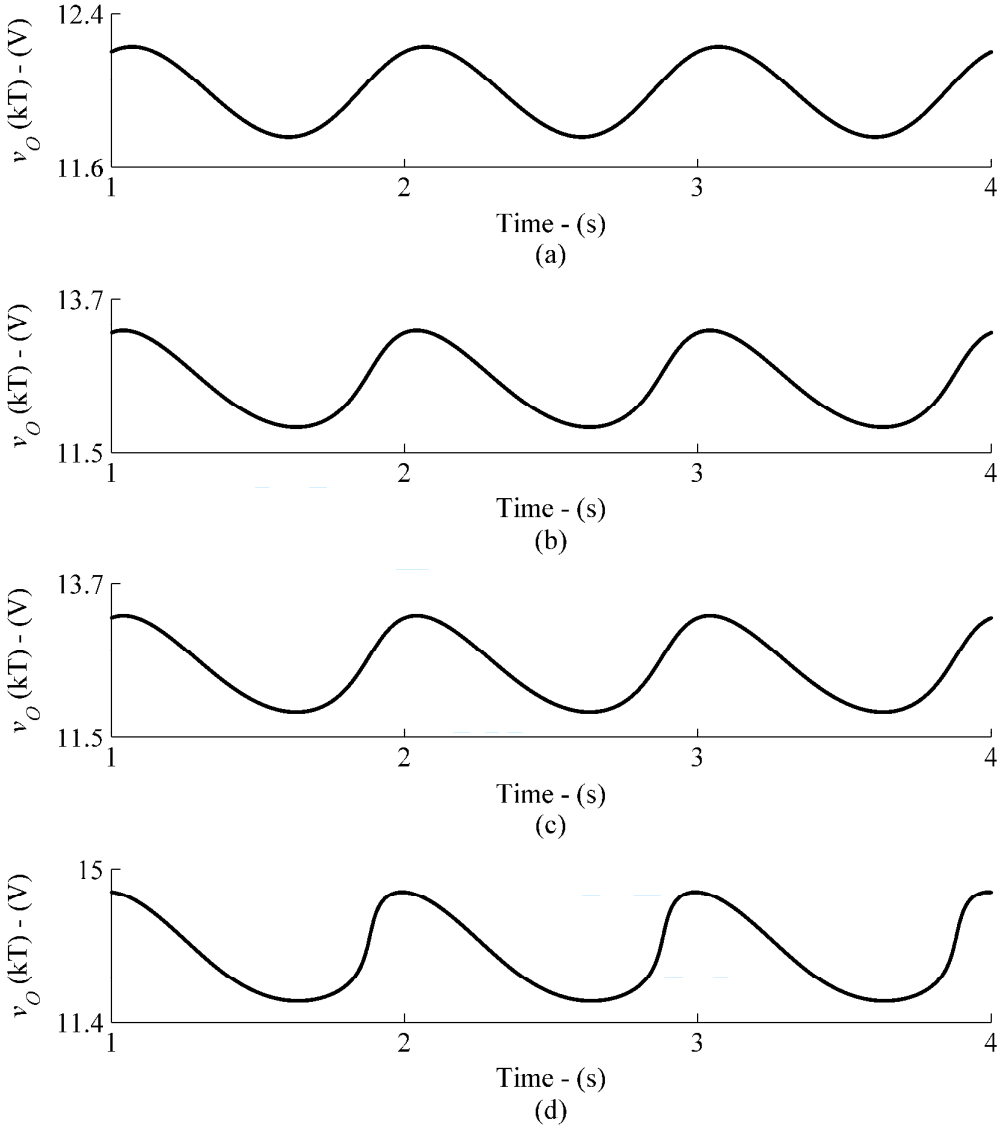

Fig. 12: Time-bifurcation plots of the output voltage for $f_n = 2499$ (Hz) using the k_u values presented in Table 2 (a) for (a) $\alpha_v = 0.16$ (b) $\alpha_v = 0.38$ (c) $\alpha_v = 0.5$ and (d) $\alpha_v = 1$.

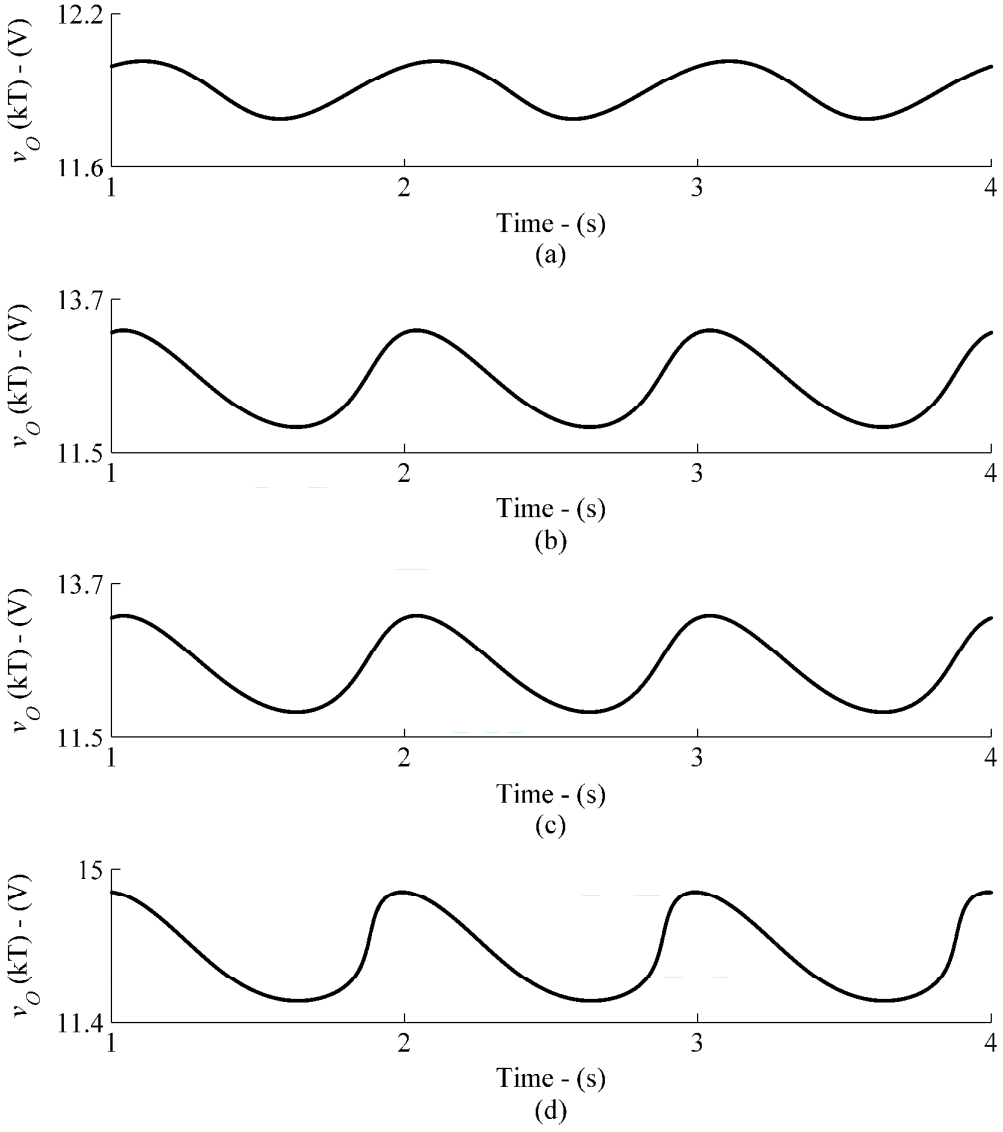

Fig. 13: Time-bifurcation plots of the output voltage for $f_n = 5001$ (Hz) using the k_u values presented in Table 2 (c) for (a) $\alpha_v = 0.16$ (b) $\alpha_v = 0.57$ (c) $\alpha_v = 0.7$ and (d) $\alpha_v = 1$.

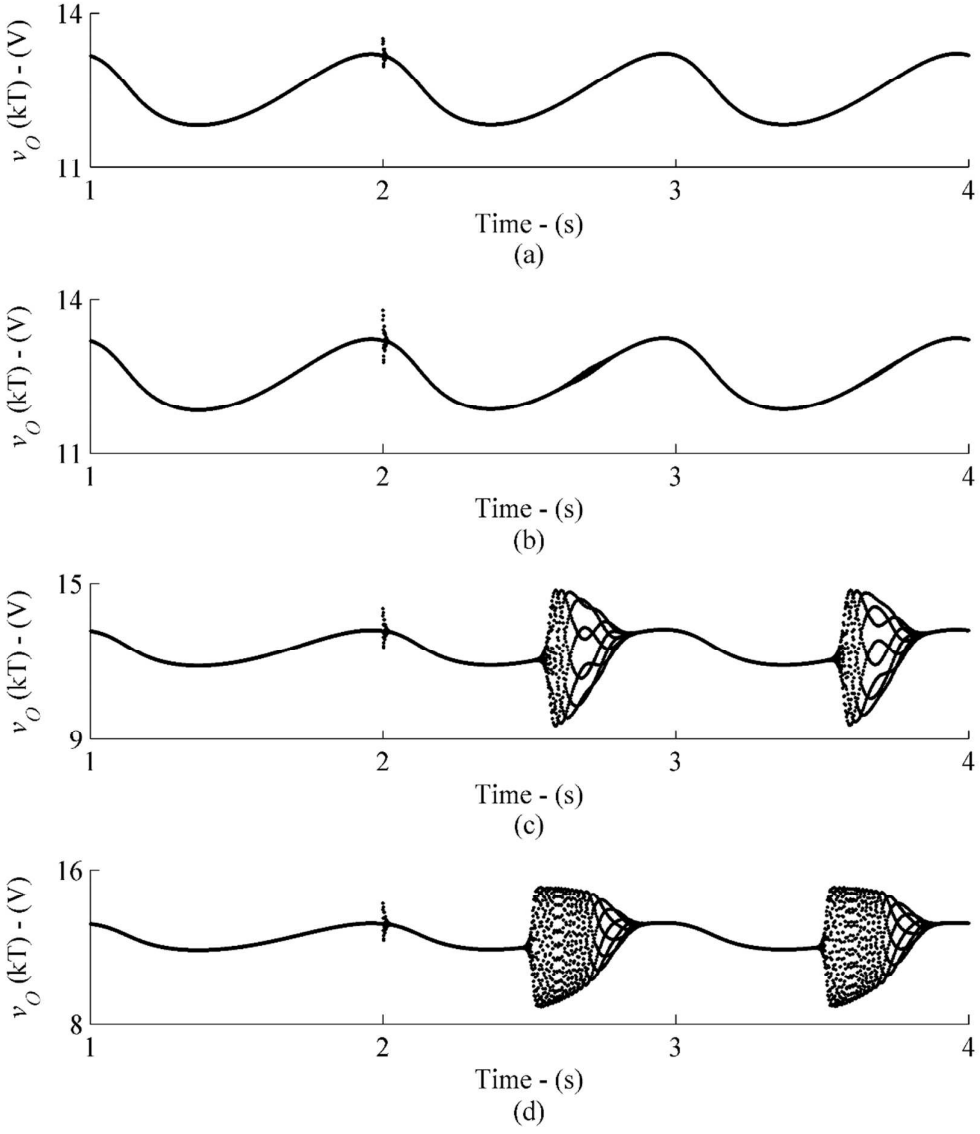

Fig. 14: Effect of variation of the load resistance on the output voltage for an increase in R by (a) 10% (b) 20% (c) 30% and (d) 40% for $f_n = 2501$ (Hz) and $\alpha_v = 0.5$.

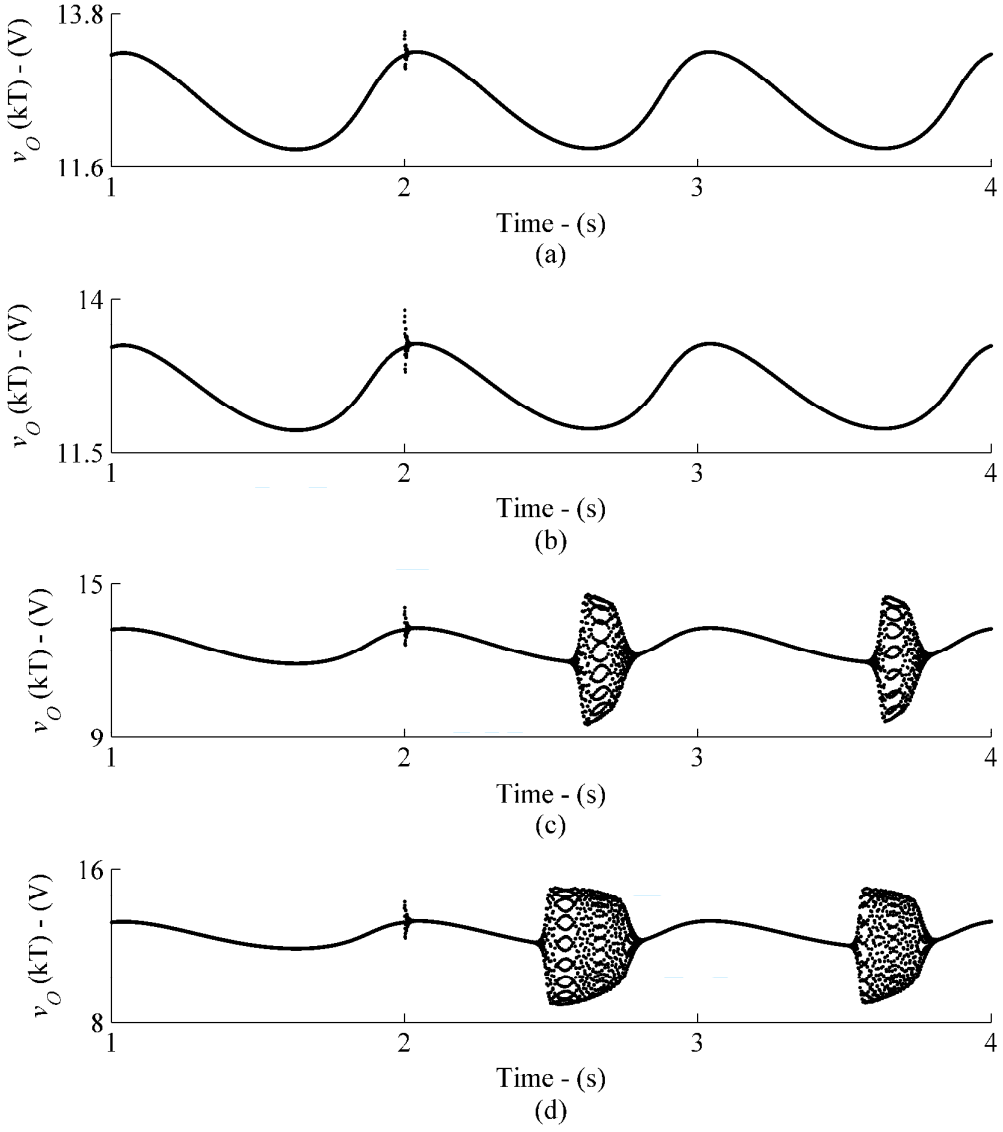

Fig. 15: Effect of variation of the load resistance on the output voltage for an increase in *R* by (a) 10% (b) 20% (c) 30% and (d) 40% for $f_n = 2499$ (Hz) and $\alpha_v = 0.5$.

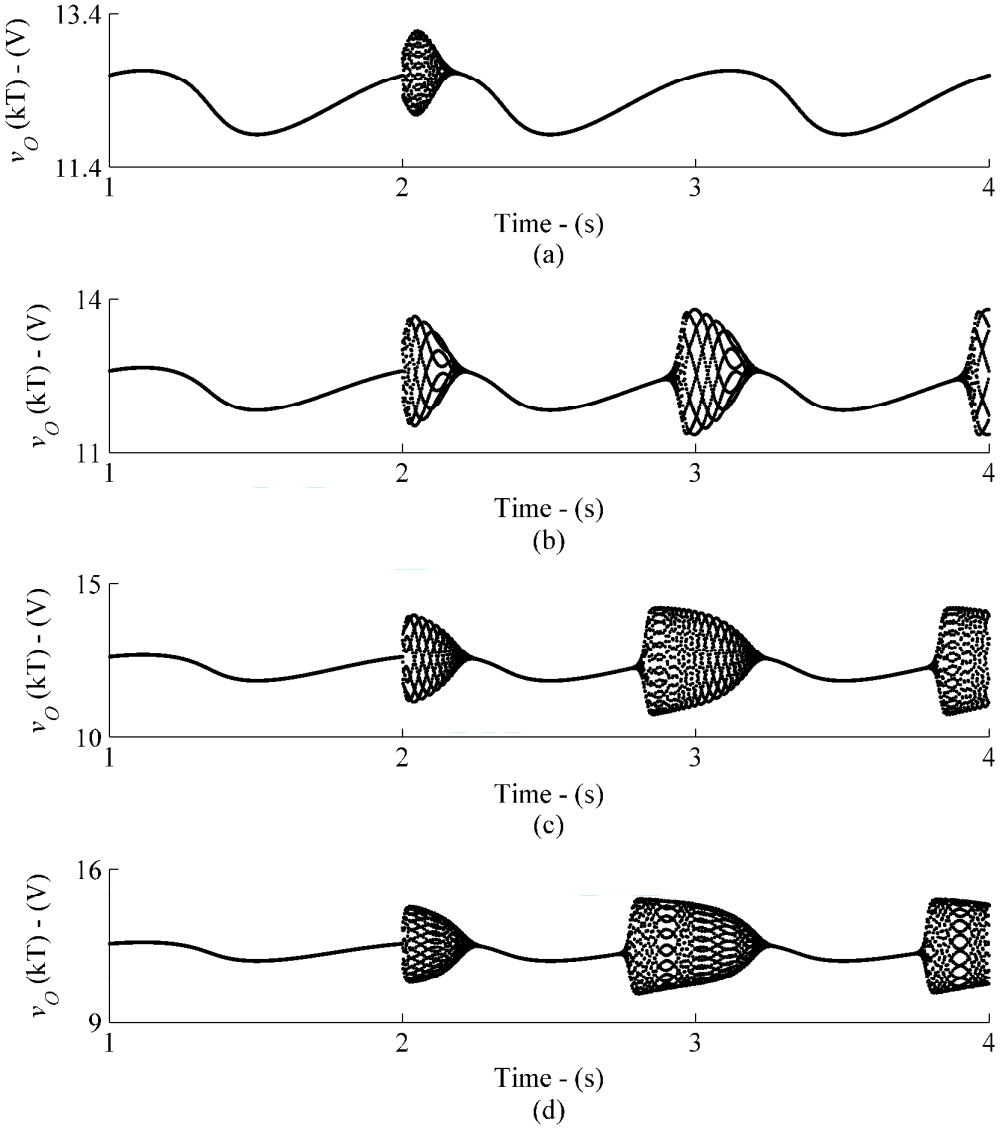

Fig. 16: Effect of variation of the load resistance on the output voltage for an increase in *R* by (a) 10% (b) 20% (c) 30% and (d) 40% for $f_n = 5001$ (Hz) and $\alpha_v = 0.57$.

6 Acknowledgements

This material is based upon works supported by Dublin City University under the Daniel O'Hare Research Scholarship scheme.

7 Conclusion

In this work, detailed analytical and numerical work has been carried out to investigate how the loss in stability of a digital state feedback controlled buck converter can lead to intermittent operation due to the presence of an undesired noise signal. The intermittent operation was characterised by a loss in stability as time varied and a limit cycle was present on the output for periods of time interspersed with periods of stable operation. Time-bifurcation plots were used to demonstrate this. It was shown that intermittent operation is more likely to occur when the frequency of the noise is close to the switching frequency. However, conventional stability analysis techniques are not suited to time-bifurcation analysis hence, a transformation was performed to convert changes in time to changes in another parameter ϕ. This enabled the application of the Filippov method to derive the Floquet Multiplier and track the eigenvalues as ϕ varied as well as deriving conditions for the elimination of the intermittent operation. Based on this, a design procedure was proposed in order to tune a controller in order to avoid intermittent operation. The buck converter under digital state-feedback control was taken as a case study. Through the use of a supervising controller, whose function was to monitor the input voltage, the procedure was shown to be effective at tuning the k_u term in an adaptive controller. Intermittent operation was eliminated. The sensitivity of the controller to variations in the load resistance was checked through simulation. It was shown that the controller effectively removed intermittent operation for 20% variations in the nominal load resistance. However, this design procedure is suitable for developing guidelines for any controller type to ensure stable operation by modifying the relevant steps in the design procedure.

References

1. Erickson R, Maksimovic, D. *Fundamentals of Power Electronics*. Dordrecht: Kluwer Academic Publishers Group 2000.

2. Giaouris D, Yfoulis C, Stergiopoulos F, Ziogou C, Voutetakis S, Papadopoulou S. Border collisions and chattering in state feedback controlled boost converters. *The International Symposium on Nonlinear Theory and its Applications 2014.*

3. Giaouris D, Yfoulis C, Voutetakis S, Papadopoulou S. Stability analysis of digital state feedback controlled boost converters. *Proceedings of the 39th Conference of the IEEE Industrial Electronics Society 2013* : 8391-8396.

4. Giaouris D, Yfoulis C, Voutetakis S, Papadopoulou S. Stability analysis of state feedback controlled boost converters. *Proceedings of the 39th Conference of the IEEE Industrial Electronics Society 2013* : 8383-8388.

5. Li ZP, Zhou Y, Chen JN. Complex intermittency in voltage-mode controlled buck converter. *Proceedings of CES/IEEE 5th International Power Electronics and Motion Control Conference 2006* : 1-5.

6. Deivasundari P, Uma G, Murali K. Chaotic dynamics of voltage-mode controlled buck converter with periodic interference signals. *International Journal of Bifurcation and Chaos* 2013; **23(1)** : 1-12.

7. Tse CK, Zhou Y, Lau FCM, Qiu SS. Intermittent chaos in switching power supplies due to unintended coupling of spurious signals. *Proceedings of the IEEE 34th Annual Power Electronics Specialists Conference, 2003* : 642-647.

8. Zhou Y, Chen JN, Iu HHC, Tse CK. Complex intermittency in switching converters. *International Journal of Bifurcation and Chaos* 2008; **18(1)** : 121-140.

9. Jiang XD, Zhou Y, Chen JN, Wang S. Intermittent chaos and subharmonic in current-mode controlled SEPIC converters. *Proceedings of the IEEE Conference on Industrial Electronics and Applications* 2008 : 833-836.

10. Cervantes I, Fermant R. Intermittent operation of linear driven switched systems. *International Journal of Bifurcation and Chaos* 2008*;* **18(2)** : 495-508.

11. Wong SC, Tse CK, Tam KC. Spurious modulation on current-mode controlled dc/dc converters: an explanation for intermittent chaos. *Proceedings of the IEEE Symposium on Circuits and Systems* 2004; **5** : 852-855.

12. Wong SC, Tse CK, Tam KC. Intermittent chaotic operation in switching power converters. *International Journal of Bifurcation and Chaos* 2004; **14(8)** : 2971-2978.

13. Murlai K, Deivasundari P, Uma G, Vincent C. Non-linear intermittent instabilities and their control in an interleaved dc/dc converter. *IET Power Electronics* 2014; **7(5)** : 1235-1245.

14. Deivasundari P, Geetha R, Uma G, Murali K. Chaos, bifurcation and intermittent phenomena in dc-dc converters under resonant parametric perturbation. *The European Physic Journal Special Topics* 2013; **222(3)** : 689-698.

15. Giaouris D, Maity S, Banerjee S, Pickert V, Zahawi B. Application of Filippov method for the analysis of subharmonic instability in dc-dc converters. *International Journal of Circuit Theory and Applications* 2009; **37(8)** : 899-919.

16. Bradley M. *Nonlinear Dynamics of Digitally-Controlled Buck Converters*. PhD dissertation, University College Dublin.

17. Hayes B, Condon M, Giaouris D. Design of PID controllers using Filippov's method for stable operation of dc-dc converters. *International Journal of Circuit Theory and Applications* 2015;

18. Bradley M, Feely O, Teplinsky A. Limit cycles in a digitally controlled buck converter. *Proceedings of the 20th European Conference on Circuit Theory and Design* 2011 : 246-249.

19. Texas Instruments. Basic Calculation of a Buck Converter's Power Stage [Online]. Available: http://www.ti.com/lit/an/slva477b/slva477b.pdf. [Accessed: 09-May-2016].

20. Maxim Integrated. Input and Output Noise in Buck Converters Explained [Online]. Available: https://www.maximintegrated.com/en/app-notes/index.mvp/id/986. [Accessed: 16-Dec-2015].

21. Filippov A, Arscott FM. *Differential equations with discontinuous righthand sides*. Kluwer, 1988.

22. Hilborn RC. *Chaos and nonlinear dynamics: an introduction for scientists and engineers.* Oxford University Press, 1994.

23. Stefanutti W, Mattavelli P, Saggini S, Ghioni M. Autotuning of Digitally Controlled Buck Converters Based on Relay Feedback. *36th IEEE Power Electronics Specialists Conference* 2005 ; 2140 – 2145.

24. Corradini L, Mattavelli P, Maksimovic D. Robust Relay-Feedback Based Autotuning for DC-DC Converters. *Power Electronics Specialists Conference* 2007 ; 2196 – 2202.

25. Kelly A, Rinne K. A self-compensating adaptive digital regulator for switching converters based on linear prediction. *21st IEEE Applied Power Electronics Conference and Exposition* 2006 ; 712 – 718.

Table 1: Eigenvalues at bifurcation point for $f_n = 2501$ (Hz).

$f_n = 2501$			
α_v	ϕ	$\lambda_{1,2}$	$\lvert\lambda_{1,2}\rvert$
0.38	2.0106	$0.7515 \pm 0.6578i$	0.9987
	2.0735	$0.7510 \pm 0.6627i$	1.0016
	4.6496	$0.7168 \pm 0.6974i$	1.0000
	4.7124	$0.7251 \pm 0.6876i$	0.9993
0.50	1.8221	$0.7549 \pm 0.6558i$	0.9999
	1.8850	$0.7535 \pm 0.6588i$	1.0009
	4.9637	$0.7167 \pm 0.6973i$	1.0000
	5.0265	$0.7169 \pm 0.6930i$	0.9971
1.00	1.4451	$0.7611 \pm 0.6248i$	0.9847
	1.5080	$0.7613 \pm 0.6486i$	1.0001
	5.7805	$0.6725 \pm 0.7403i$	1.0002
	5.8434	$0.6716 \pm 0.7366i$	0.9967

Table 2: k_{u_crit} for varying signal strengths and noise frequencies

(a)

f_n	α_v	k_{u_crit}
2501	0.16	0.0110
	0.38	0.0010
	0.50	-0.0027
	1.00	-0.0151

(b)

f_n	α_v	k_{u_crit}
2499	0.16	0.0100
	0.38	0.0004
	0.50	-0.0037
	1.00	-0.0155

(c)

f_n	α_v	k_{u_crit}
5001	0.16	0.0121
	0.38	0.0002
	0.50	-0.0045
	1.00	-0.0098

Appendix A: Derivation of $x(kT)$

SW_1 is closed at the start of the switching period and remains closed for dT. The switching is closed from $kT \to (k+d)T$. Therefore, (2) becomes:

$$\int_{kT}^{(k+d)T} \frac{d}{dt}\left(e^{-At}x\right)dt = \int_{kT}^{(k+d)T} e^{-At}BV_{IN}dt$$

However, $V_{IN} = V_{IN}^*\left(1+\alpha_v \sin\left(2\pi f_n t\right)\right)$:

$$x\left((k+d)T\right) = e^{AdT}x\left(kT\right) - A^{-1}\left(I - e^{AdT}\right)BV_{IN}^* + \alpha_v e^{A(k+d)T}\int_{kT}^{(k+d)T} e^{-At}\sin\left(2\pi f_n t\right)dt\, BV_{IN}^* \quad \text{(A.1)}$$

Let $N_{dT} = e^{A(k+d)T}\int_{kT}^{(k+d)T} e^{-At}\sin\left(2\pi f_n t\right)dt$. Using integration by parts, N_{dT} can be derived to be:

$$N_{dT} = e^{A(k+d)T}\left(A^2 + \left(2\pi f_n\right)^2\right)^{-1}\left(-Ae^{-At}\sin\left(2\pi f_n t\right) - 2\pi f_n e^{-At}\cos\left(2\pi f_n t\right)\right)\Big|_{t=kT}^{t=(k+d)T}$$

Inserting the limits yield:

$$N_{dT} = \left(A^2 + (2\pi f_n)^2\right)^{-1}\left(Ae^{AdT}\sin\left(2\pi f_n kT\right) + 2\pi f_n e^{AdT}\cos\left(2\pi f_n kT\right) - AI\sin\left(2\pi f_n (k+d)T\right) - 2\pi f_n I\cos\left(2\pi f_n (k+d)T\right)\right)$$

Evaluating (A.1), the state variable at the start of the switching period can be related to the state variable at the switching instant:

$$x\left((k+d)T\right) = e^{AdT}x\left(kT\right) - A^{-1}\left(I - e^{AdT}\right)BV_{IN}{}^* + \alpha_v N_{dT}BV_{IN}{}^* \quad \text{(A.2)}$$

Rearranging (A.2) so that the value of the state vector at the start of the switching period is expressed in terms of its value at the switching instant gives:

$$x(kT) = e^{-AdT}x\left((k+d)T\right) + A^{-1}\left(e^{-AdT} - I\right)BV_{IN}^{\ *} + \alpha_v N_{kT} BV_{IN}^{\ *} \tag{A.3}$$

where:

$$N_{kT} = \left(A^2 + (2\pi f_n)^2\right)^{-1} \left(-AI\sin(2\pi f_n kT) - 2\pi f_n I\cos(2\pi f_n kT) + Ae^{-AdT}\sin(2\pi f_n(k+d)T) + 2\pi f_n e^{-AdT}\cos(2\pi f_n(k+d)T)\right)$$